Lnc-RGS5 sponges miR-542-5p to promote FoxM1/VEGFA signaling and breast cancer cell proliferation

JING SONG*, YONGYAO TANG* and FANGZHOU SONG

Molecular and Tumor Research Center, The Basic Medical School of Chongqing Medical University, Chongqing 400016, P.R. China

Received April 12, 2023; Accepted July 26, 2023

DOI: 10.3892/ijo.2023.5559

Abstract. Breast cancer (BRCA) exhibits a high incidence rate among women worldwide. LOC127814295 (ENSG00000232995), termed long non-coding (lnc)-regulator of G protein signaling 5 (RGS5), is a novel lncRNA with a genomic region overlapping with protein-coding gene RGS5. Results obtained using The Cancer Genome Atlas demonstrated that lnc-RGS5 was deregulated in diverse cancer types, including BRCA; however, the functional role of lnc-RGS5 remains unclear. Results of the present study demonstrated that lnc-RGS5 was upregulated in BRCA tissues compared with healthy samples (n=30; P<0.0001), and was associated with the overall survival of patients with triple-negative BRCA (n=106; P<0.05). Moreover, lnc-RGS5 expression was significantly higher in triple-negative BRCA samples than in LumA, LumB, or Her2 subtypes (P<0.05). Functionally, lnc-RGS5 upregulation promoted BRCA cell proliferation *in vitro*, whereas lnc-RGS5 knockdown elicited the opposite function. Stable knockdown of lnc-RGS5 inhibited tumor cell proliferation *in vivo*. Bioinformatics analysis revealed that lnc-RGS5 was significantly associated with RNA binding involved in post-transcriptional gene silencing (P=0.002). Mechanistically, lnc-RGS5 functions as a competing endogenous RNA via competitively sponging miR-542-5p to upregulate forkhead box M1 (FoxM1) and the VEGFA/Neuropilin 1 axis; thus, promoting BRCA cell proliferation *in vitro*. Moreover, rescue experiments validated that the lnc-RGS5/miR-542-5p/FoxM1 axis promoted BRCA cell growth *in vivo*. Collectively, results of the present study demonstrated that lnc-RGS5 may exhibit potential as a novel oncogenic lncRNA in BRCA. The present study may provide a novel theoretical basis for the role of lncRNA in the targeted therapy of BRCA.

Correspondence to: Dr Fangzhou Song, Molecular and Tumor Research Center, The Basic Medical School of Chongqing Medical University, 1 Yixueyuan Road, Yuzhong, Chongqing 400016, P.R. China
E-mail: fzsong@cqmu.edu.cn

*Contributed equally

Key words: breast cancer, tumorigenesis, competing endogenous RNA, proliferation

Introduction

Breast cancer (BRCA) is the most common cancer in women worldwide. In total, >43,000 BRCA-related deaths are estimated in 2023 (1), and this may be due to a high degree of tumor heterogeneity. The histological subtypes of BRCA observed in clinical practice are Her2 (ER^-, PR^-, $HER2^+$), LumA (ER^+/PR^+, $HER2^-$), LumB (ER^+/PR^+, $HER2^+$) and triple-negative BRCA (ER^-, PR^-, $HER2^-$). Although a further understanding of BRCA subtypes has led to improved outcomes using targeted therapies, patients with triple-negative BRCA exhibit a poor prognosis due to augmented proliferative activity and acquired treatment resistance (2). Numerous drugs targeting the cell cycle have been developed to inhibit augmented proliferative activity, including gemcitabine, a chemotherapeutic agent for G1/S phase, and tyrosine kinase inhibitors, such as CDK4/6 (3). However, acquired treatment resistance to the aforementioned drugs was observed in patients following therapy (4,5). Notably, triple-negative BRCA may also be treated using anti-vascular endothelial growth factor (VEGF) therapy, including Avastin and Lucentis, which inhibit proliferative activity and angiogenesis. However, decreased tumor vessel and drug penetration, and increased hypoxia stimulated increased VEGF expression, resulting in resistance (6,7). Thus, the development of novel therapeutic targets is required to overcome the excessive proliferation and drug resistance of BRCA.

Long non-coding RNAs (lncRNAs), exhibit no coding potential and are >200 nucleotides in length. Notably, lncRNAs play a critical role in BRCA. For example, the upregulation of H19 inhibited the binding of DNA methyltransferase 3 β (DNMT3B) to the Beclin1 promoter region, resulting in tamoxifen resistance in BRCA cells. Moreover, H19 knockdown reversed this effect (8). In addition, LINC00511 promoted the proliferation of BRCA cells via sponging miR-185-3p to activate E2F transcription factor 1/Nanog signaling (9). Notably, lncRNA may be divided into numerous subgroups according to the location on the genome, including intronic, intergenic, divergent and antisense lncRNA. Thus, lncRNA and protein-coding transcripts may overlap in the genome but exhibit different functions. GATA binding protein

3 (GATA3) transcription activates Semaphorin 3B to inhibit BRCA development (10). By contrast, GATA3-AS1 destabilized the GATA3 protein, and enhanced the progression and immune escape of triple-negative BRCA through promoting GATA3 ubiquitination (11).

LOC127814295 [known as lnc-regulator of G protein signaling 5 (RGS5) or ENSG00000232995] is a novel lncRNA with a genomic region overlapping with protein-coding gene RGS5. As a protein-coding gene, RGS5 is involved in tumor development and tumor microenvironment remodeling. Results of a previous study demonstrated that the RGS5-TGFβ-PSmad2 axis reduces RGS5- and TGFβ-dependent cell apoptosis through promoting PI3K-AKT signaling, and preventing mitochondrial damage and activation of caspases. This process leads to sustained pericyte survival and expansion in the tumor microenvironment (12). Notably, RGS5 promotes the occurrence of tumor angiogenesis in the tumor microenvironment of human melanoma and renal cancer xenografts (13). In addition, RGS5 exhibits potential as a widely expressed tumor antigen for identifying and characterizing T cell epitopes (14). However, studies focusing on the specific role of lnc-RGS5 in cancer are lacking, despite the deregulation of lnc-RGS5 in numerous cancer types. Therefore, the present study aimed to investigate the functional role of lnc-RGS5 and determine the clinical implications in BRCA. The present study also aimed to further elucidate the mechanistic role of lnc-RGS5 in regulating BRCA proliferation.

Materials and methods

Patient tissues and ethics approval. A total of 30 pairs of tissues from patients with BRCA were collected from The First Affiliated Hospital of Chongqing Medical University (Chongqing, China). Written informed consent was obtained from all patients. Women patients who were diagnosed with BRCA by two pathologists were included in the study (October 1, 2020 to December 30, 2020). All experimental procedures were approved by Ethics Committee of Chongqing Medical University (Chongqing, China) (approval date: September 20, 2020). Informed consent was obtained from all patients.

Analysis of gene expression and survival in public databases. Gene expression was analyzed in diverse cancer types detailed in The Cancer Genome Atlas (TCGA) database (https://portal.gdc.cancer.gov/). A comparison of gene expression between tumors and healthy samples was performed using the DESeq2 package (15) in R (version 4.2.3; https://www.r-project.org/). The expression correlation between gene pairs was performed using Pearson's correlation coefficient based on TCGA-BRCA dataset (https://portal.gdc.cancer.gov/projects/TCGA-BRCA). Benjamini-Hochberg adjusted P<0.05 was used as a threshold. Kaplan-Meier survival analysis was performed for triple-negative BRCA based on TCGA-BRCA dataset using R software (v4.2.3). Log-rank test was used for survival analysis and P<0.05 was used as a threshold. Median as cut-off was used.

Gene set enrichment analysis (GSEA). The Gene Ontology (GO) functions and Kyoto Encyclopedia of Genes and Genomes pathways of lnc-RGS5 were analyzed using GSEA software (16). Patients were divided into high and low lnc-RGS5 expression groups according to the median expression of lnc-RGS5. Nominal P<0.05 was used as a threshold.

Regulation network analysis. A regulation network was constructed based on the putative interactions of genes. lnc-RGS5 and miRNA interactions, and miRNA-coding gene interactions were determined based on RNAhybrid (17) and miRanda (18) software. Notably, genes that interacted with miRNAs are often negatively correlated with miRNAs. Only genes differentially expressed in BRCA were considered. For transcription factors, putative targets were obtained from the Gene Transcription Regulation Database (GTRD) database (19).

Cell lines and culture. MCF-7 and MDA-MB-231 cell lines were purchased from the American Type Culture Collection (ATCC), and cultured in complete DMEM (Gibco; Thermo Fisher Scientific, Inc.) containing 10% fetal bovine serum (FBS; Shanghai ExCell Biology, Inc.), 100 U/ml penicillin and 0.1 mg/ml streptomycin (Beyotime Institute of Biotechnology) at 37˚C in a humidified atmosphere containing 5% CO_2.

Cell transfection. Small interfering RNA (siRNA) targeting lnc-RGS5 and the negative control (NC) were purchased from Shanghai GenePharma Co., Ltd. Micro (mi)RNA inhibitor and mimics were purchased from Tsingke Biological Technology. Following the manufacturer's instructions, cells were transfected using siRNA-Mate (Shanghai GenePharma Co., Ltd.). The pcDNA3.1/forkhead box M1 (FoxM1) and pcDNA3.1/lnc-RGS5 plasmids were purchased from Tsingke Biological Technology and cells were transfected using Lipofectamine® 2000 (Invitrogen; Thermo Fisher Scientific, Inc.). Cells were transfected with siRNAs (1 μg) or plasmids (2 μg) and cultured at 37˚C for 48 h to perform subsequent experiments. Sequences were as follows: silnc-RGS5-1, 5'-UUUAAAGUGCAGUCUCUGUAC-3'; silnc-RGS5-2, 5'-UUUAAUGCCAUCCUGGCCAGA-3'; silnc-RGS5-3, 5'-UUUAAACAGGUGAUCCCUAGA-3'; siFoxM1, 5'-GGACCACUUUCCCUACUUU-3'; siNC, 5'-UUCUCCGAACGUGUCACGUTT-3'; miR-542-5p inhibitor, 5'-UCUCGUGACAUGAUGAUCCCCGA-3'; NC inhibitor, 5'-UCUACUCUUUCUAGGAGGUUGUGA-3'; miR-542-5p mimics, 5'-UCGUGACAUGAUGAUCCCCGAUU-3'; and NC mimics, 5'-UCACAACCUCCUAGAAAGAGUAGA-3'.

RNA extraction and reverse transcription-quantitative (RT-q) PCR. Total RNA was extracted from MCF-7 and MDA-MB-231 cells using TRIzol® reagent (Invitrogen; Thermo Fisher Scientific, Inc.) according to the manufacturer's instructions. RNA (500 mg) was reverse transcribed into a 10 μl final volume of cDNA using Reverse Transcription kit (Takara Bio, Inc.), following the manufacturer's instructions. lnc-RGS5 and miR-542-5p RNA expression were measured using qPCR on the Step One Plus Real-Time PCR system. qPCR was conducted in three independent experiments using SYBR® Premix Ex Taq™ II (Takara Bio, Inc.) and analyzed using the $2^{-\Delta\Delta Cq}$ method (20). qPCR reaction conditions were as follows: Initial denaturation at 95˚C for 30 sec, followed by 39 cycles at 95˚C for 5 sec and 60˚C for 30 sec. GAPDH and U6 were used as endogenous controls. The

primers were designed by Tsingke Biological Technology. qPCR primer sequences were as follows: GAPDH forward, 5'-CCA TGGGGAAGGTGAAGGTC-3' and reverse, 5'-AGTGATGGC ATGGACTGTGG-3'; U6 forward, 5'-GCTTCGGCAGCACAT ATACTAAAAT-3' and reverse, 5'-CGCTTCACGAATTTG CGTGTCAT-3'; lnc-RGS5 forward, 5'-AGTGACAAGATG GGGGTGTTC-3' and reverse, 5'-CTGGTGGCTTCTGTTGGT TTG-3'; miR-542-5p forward, 5'-TCGGGGATCATCATGT-3' and reverse, 5'-GTGCAGGGTCCGAGGT-3'; and miR-542-5p, 5'-GTCGTATCCAGTGCAGGGTCCGAGGTATTCGCACTG GATACGACCTGCGGTCTCGTG-3'.

Western blot analysis. MCF-7 and MDA-MB-231 cells were transfected with miRNA and siRNA and cultured for 48 h. Total protein was extracted from cells using lysis buffer (cat. no. KGP250; Keygene Biotech, Inc.; http://www.keygentec.com.cn/), and the protein concentration was measured using Enhanced BCA Protein Assay Kit (cat. no. P0010; Beyotime Institute of Biotechnology). A total of 40 μg proteins were loaded per lane in SDS-PAGE. Proteins were separated via SDS PAGE on a 10% gel. The separated proteins were subsequently transferred onto PVDF membranes. The membranes were then blocked with 5% non-fat milk in TBST (1 ml/l Tween-20; cat. no. ST825; Beyotime Institute of Biotechnology) at room temperature (RT) for 1 h, and incubated with the following primary antibodies: Anti-β-actin (1:1,000; cat. no. 20536-1-AP; ProteinTech Group, Inc.), anti-FoxM1 (1:1,000; cat. no. ab207298; Abcam), anti-VEGFA (1:1,000; cat. no. ab214424; Abcam) and anti- Neuropilin 1 (NRP1; 1:1,000; cat. no. ab81321; Abcam) overnight at 4˚C. Following primary incubation, membranes were incubated with the HRP-conjugated secondary antibody (1:5,000; cat. no. SA00001-2; ProteinTech Group, Inc.) at RT for 1 h. The protein ladder was purchased from Shanghai Epizyme Biomedical Technology Co., Ltd. (cat. no. WJ103; 10~250 kDa). Protein bands were visualized using the Pierce ECL Plus Western Blotting Substrate (Bio-Rad Laboratories, Inc.). Protein expression was quantified using ImageJ 5.2.1 software (National Institutes of Health) with β-actin as the loading control.

RNA immunoprecipitation assay. RNA immunoprecipitation assays were performed using a BersinBio™ RIP kit according to the manufacturer's instructions. The MCF-7 and MDA-MB-231 cells (density: ~90%) were lysed using lysis buffer containing a protease inhibitor cocktail and RNase inhibitor, and the lysates were immunoprecipitated with anti-Ago2 (5 μl; cat. no. 67934-1-Ig; ProteinTech Group, Inc.) and IgG (5 μl; cat. no. 30000-0-AP; ProteinTech Group, Inc.) antibodies at 4˚C overnight. A total of 30 μl Protein A-Agarose beads (cat. no. sc-2001; Santa Cruz Biotechnology, Inc.) were added and incubated at 4˚C for 2 h. After centrifugation at 200 x g for 30 sec, beads were 3 times washed with wash buffer (20 mM Tris-HCl pH 8.0, 200 mM NaCl, 1 mM EDTA, 0.5% Triton X-100, 0.4 U/μl RNase inhibitor, and 0.4 U/μl Protease Inhibitor Cocktail). The retrieved RNAs were quantified using RT-qPCR.

Dual-luciferase reporter assay. Transfection and luciferase reporter assays were performed as previously described (21). lnc-RGS5 cDNA containing the predictive binding site of miR-542-5p was cloned into the pmirGLO Dual-Luciferase miRNA Target Expression Vector (Promega Corporation) to form the wild-type vector (lnc-RGS5-WT). Mutant (Mut) lnc-RGS5 containing mutations of the miR-542-5p binding site was specifically synthesized and inserted into the aforementioned vector (lnc-RGS5-Mut). BRCA cells were cultured and co-transfected with pmirGLO-lnc-RGS5-3'-untranslated region (UTR) vectors, including WT or Mut fragments and miR-542-5p mimics. The pmirGLO vector was used as the NC. FoxM1-WT and FoxM1-Mut were cloned into the pmirGLO vector (Promega Corporation) using the one-step directed cloning kit (Novoprotein Scientific, Inc.). miR-542-5p mimics were co-transfected with FoxM1-WT or FoxM1-Mut vector into BRCA cells using Lipofectamine® 2000 (Invitrogen; Thermo Fisher Scientific, Inc.). Luciferase activity was evaluated using Dual-Luciferase® Reporter Assay System (Promega Corp.) after 48-h transfection. Data were presented as a ratio of Firefly to *Renilla* luciferase activity.

Short hairpin (sh)RNA transfection. shRNA targeting lnc-RGS5 (shlnc-RGS5 sequence, 5'-GCATGGTTGGAGACAATAAGT CTCGAGACTTATTGTCTCCAACCATGC-3'; target sequence, 5'-GCATGGTTGGAGACAATAAGT-3'; 1 μg) was expressed using the pLKO.1-TRC-copGFP-T2A-Puro vector (TsingKe Biological Technology). A scrambled shRNA (5'-TTCTCCGAA CGTGTCACGT-3'; 1 μg) was used as a negative control (shNC). MDA-MB-231 cells expressing green fluorescent protein were screened after 72 h transfection at 37˚C. HiTransG P transfection agent (Shanghai Genechem Co., Ltd.) was used. To generate stable lnc-RGS5-knockdown cells, 2 μg/ml puromycin was used for induction, and 1 μg/ml puromycin was used for maintenance.

Cell viability and proliferation assay. A Cell Counting Kit-8 (CCK-8) assay (cat. no. 40203ES60; Shanghai Yeasen Biotechnology Co., Ltd.) was used to measure cell proliferation. In total, 2,000 cells were seeded in 96-well plates, and 10 μl CCK-8 solution was diluted and added. After incubation with CCK-8 reagent at 37˚C for 1 h in dark, absorbance was measured at 450 nm. Cell proliferation was also detected using a BeyoClickTM EdU Cell proliferation kit according to the manufacturer's instructions (Beyotime Institute of Biotechnology). Cells were stained with Alexa Fluor 488 at RT for 30 min in dark, and observed using a fluorescence microscope using a 10X objective lens (magnification, x100; Nikon Eclipse Ts2R; Nikon Corporation).

RNA expression in the nucleus and cytoplasm. RNA was extracted from the nuclei and cytoplasm using the PARIS kit (Thermo Fisher Scientific, Inc.), according to the manufacturer's instructions. An RNase inhibitor was used in RNA extraction. The purity of extracted RNA was evaluated, and high-quality RNA (260/280 nm ratio >1.8) was used for subsequent RT-qPCR experiments. U2 and β-actin were used as endogenous controls, and the primer sequences were as follows: U2 forward, 5'-CCTTTTGGCTAAGATCAAGTG TAGTATCTGTT-3' and reverse, 5'-AGCAAGCTCCTATTC CATCTCCCTG-3'; and β-actin forward, 5'-CCTTCCTGG GCATGGAGTC-3' and reverse, 5'-TGATCTTCATTGTGC TGGGTG-3'.

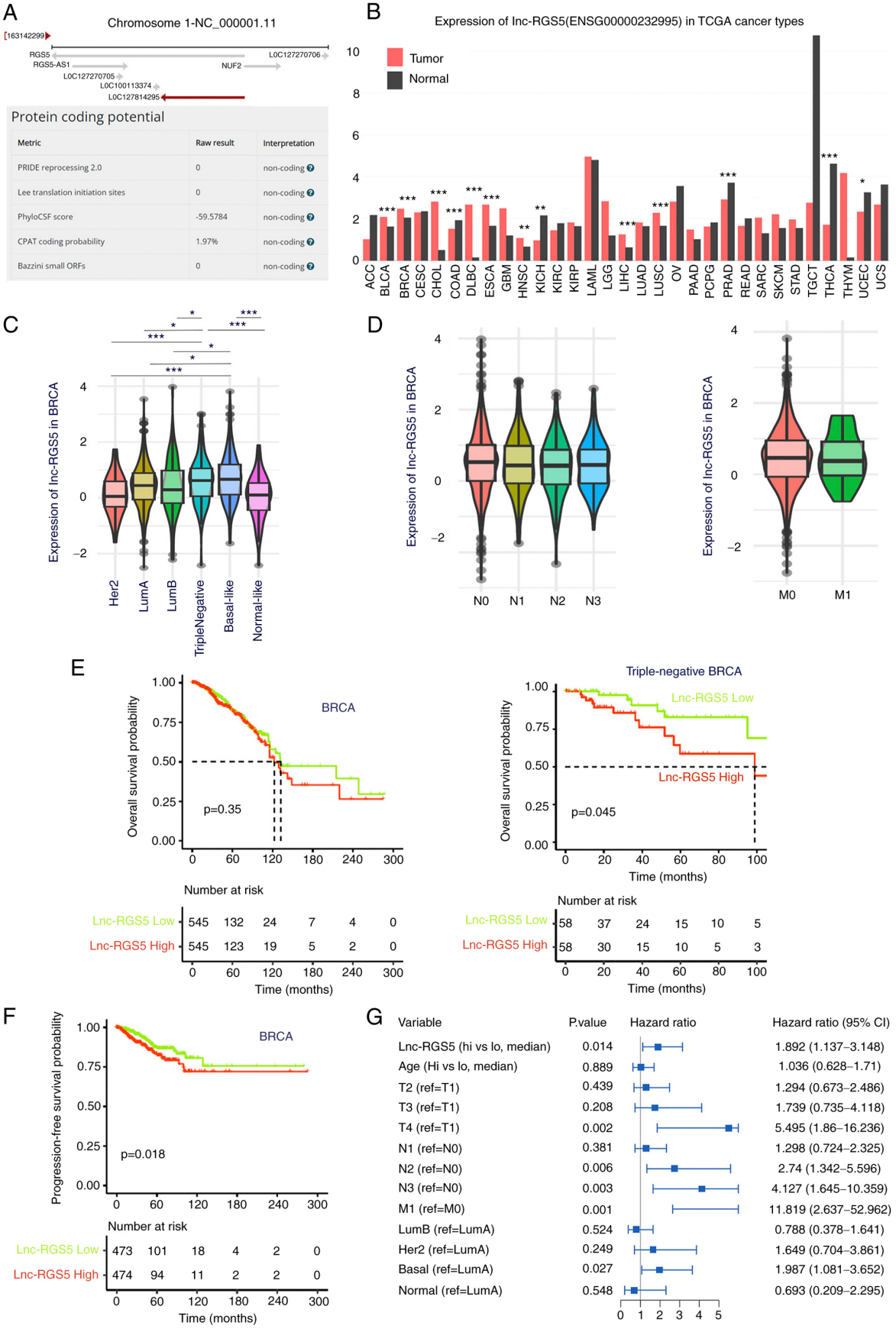

Figure 1. Expression and clinical analysis of lnc-RGS5 in BRCA. (A) Genomic location and protein-coding potential of lnc-RGS5. (B) Expression of lnc-RGS5 in TCGA cancer types. (C) Expression of lnc-RGS5 in BRCA subtypes. (D) Expression of lnc-RGS5 in patients with lymph node (N) and distant metastasis (M) compared with patients without metastasis. (E) Overall survival analysis of lnc-RGS5 in patients with BRCA and triple-negative BRCA. Median lnc-RGS5 expression was used as the cut-off value. (F and G) Univariate and multivariate progression-free survival analyses of lnc-RGS5 in patients with BRCA. *P<0.05, **P<0.01 and ***P<0.001. N1, 1-3 lymph node metastasis; N2, 4-9 lymph node metastasis; N3, >9 lymph node metastasis; M0, without distant metastasis; M1, with distant metastasis; lncRNA, long non-coding RNA; BRCA, breast cancer; TCGA, The Cancer Genome Atlas; RGS5, regulator of G protein signaling 5.

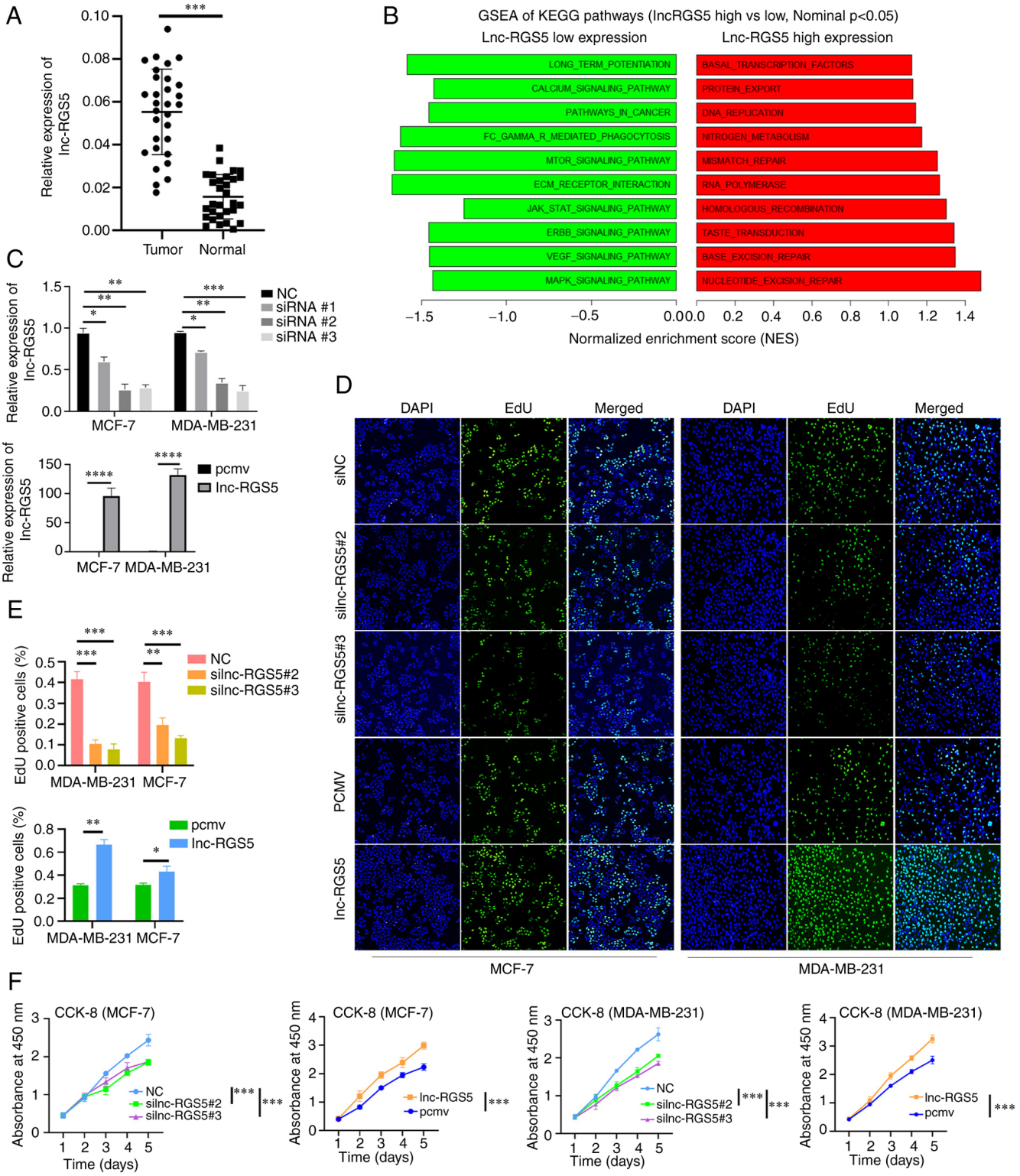

Figure 2. Upregulation of lnc-RGS5 promotes BRCA cell proliferation. (A) Expression of lnc-RGS5 in BRCA tissues and healthy tissues (n=30). (B) GSEA of KEGG pathways in high and low lnc-RGS5 expression groups. (C) Transfection efficiency of RGS5 knockdown and RGS5 overexpression. (D-F) EdU and CCK-8 assays following siRGS5 and RGS5 overexpression in MCF7 and MDA-MB-231 cells, compared with the negative control. *P<0.05, **P<0.01, ***P<0.001 and ****P<0.0001. PCMV, pcDNA3,1 empty vector; lncRNA, long non-coding RNA; BRCA, breast cancer; GSEA, gene set enrichment analysis; KEGG, Kyoto Encyclopedia of Genes and Genomes; CCK-8, Cell Counting Kit-8; RGS5, regulator of G protein signaling 5; siRNA, small-interfering RNA.

In vivo tumor formation assay. Nude BALB/c-nu mice (age, 4 weeks; sex, female; weight, 16-18 g; n=16) were purchased from Huafukang Biotechnology Company. The *in vivo* tumor formation assay was performed as previously described (22). Briefly, 6x10^{5} MDA-MB-231 cells resuspended using phosphate buffered saline (PBS) stably transfected with LV-shlnc-RGS5 or LV-NC were inoculated subcutaneously into the axillary fossa. Antagomir-542-5p and antagomir-NC (5 nmol/mouse each time), shFoxM1 (target sequence, 5'-CTCTTCTCCCTCAGATATA-3'), or shNC

plasmids (10 μg/mouse each time) were injected into the tumors every three days following tumor formation (n=4 in each group, randomly allocated). The diameter of the largest tumor observed did not exceed 1.5 cm. At the end of the experiment, all mice were sacrificed by cervical dislocation. All animal experiments were blinded and carried out in the IVC Laboratory under specific pathogen-free (SPF) conditions (4 nude mice per cage) of Barrier Facilities of Chongqing Medical University. All mice were group housed on a 12-h dark/12-h light cycle at temperatures of 18-23˚C with 40-60% humidity, and were provided with sufficient food and water. All animal experiments were reviewed and approved (approval no. IACUC-CQMU-2022-0016) by the Experimental Animal Management and Use Committee of Chongqing Medical University (Chongqing, China).

Statistical analysis. Bioinformatics analysis was conducted using R software (version 4.2.3; https://www.r-project.org/). Statistical analysis for experiment results was conducted based on three replications using Prism 8 (Dotmatics). Unpaired t-tests were used for two-group comparisons. A $P<0.05$ was considered to indicate a statistically significant difference. Error bars (mean ± standard deviation) were shown.

Results

Expression and clinical analyses of lnc-RGS5 in BRCA. In Fig. 1A, the lnc-RGS5 (*LOC127814295*) gene located on 1q23.3 is demonstrated. As a lncRNA, the transcripts of lnc-RGS5 were >200 nucleotides in length, with very low protein-coding potential (The Coding Potential Assessment Tool; CPAT software; 1.97%), no open reading frames and no translation initiation site (Fig. 1A). Results of TCGA data analysis demonstrated that lnc-RGS5 was upregulated in diverse cancer types, such as bladder cancer, esophagus cancer and BRCA (Fig. 1B). Moreover, *lnc-RGS5* expression was significantly higher in basal-like or triple-negative BRCA than in Her2 (P=0.0006), LumA (P=0.028) or LumB (P=0.048) subtypes (Fig. 1C). However, lnc-RGS5 demonstrated no significant association with lymph node or distant metastasis (P>0.05; Fig. 1D). Results of the survival analysis demonstrated that high lnc-RGS5 expression was associated with poor overall survival of patients with triple-negative BRCA (cut-off, median lnc-RGS5 expression; P=0.045; Fig. 1E) and progression-free survival (cut-off, median lnc-RGS5 expression; P=0.018; Fig. 1F) of patients with BRCA. Results of the multivariate analysis demonstrated that lnc-RGS5 may act as an independent factor for progression-free survival (Fig. 1G). These results implied that *lnc-RGS5* may play a critical role in the tumorigenesis of BRCA and may exhibit potential as a prognostic biomarker in triple-negative BRCA.

lnc-RGS5 is upregulated and increases cell proliferation in BRCA. Results of the RT-qPCR analyses indicated that *lnc-RGS5* was upregulated in BRCA compared with healthy samples (Fig. 2A, Table I). GSEA demonstrated that high lnc-RGS5 expression was associated with increased activities of DNA repair, protein export and DNA replication. By contrast, low lnc-RGS5 expression was associated with decreased activities of mTOR, MAPK, Erb-B2 Receptor Tyrosine Kinase (ERBB) and VEGF signaling pathways (Fig. 2B). Collectively, these results suggested that lnc-RGS5 may be involved in sustaining the proliferative signaling of BRCA. Thus, the role of lnc-RGS5 was further validated in BRCA cell proliferation.

Table I. The clinical information of patients with breast cancer.

Variable	Number of patients (%)
Age (median, 58 years old)	
<60	7 (23.3)
≥60	23 (76.7)
Sex	
Female	30 (100)
Tumor size (T)	
T1	10 (33.3)
T2	8 (26.7)
T3	8 (26.7)
T4	4 (13.3)
Lymph node (N)	
N0	22 (73.3)
N1	8 (26.7)
Distant metastasis (M)	
M0	16 (86.7)
M1	4 (13.3)
PAM50 Subtype	
Luminal A	10 (33.3)
Luminal B	6 (20)
Her2-enriched	5 (16.7)
Basal-like	5 (16.7)
Normal-like	4 (13.3)

In the present study, lnc-RGS5 was overexpressed and silenced following transfection with lnc-RGS5 overexpression plasmid and lnc-RGS5 siRNAs, respectively (Fig. 2C). Results of the CCK-8 and EdU assays indicated that overexpression of lnc-RGS5 promoted proliferation, while si-lnc-RGS5 transfection inhibited the growth of BRCA cells (Fig. 2D-F). These findings confirmed that lnc-RGS5 significantly enhances the growth of BRCA cells *in vitro*.

Lnc-RGS5 functions as a competing endogenous RNA (ceRNA) for miR-542-5p in BRCA. To investigate the mechanism of lnc-RGS5 in BRCA, GO enrichment analysis was performed. Results of the present study demonstrated that lnc-RGS5 was associated with RNA binding involved in post-transcriptional gene silencing (Fig. 3A), such as ceRNA mechanisms. Results of the RT-qPCR analysis revealed that lnc-RGS5 was mainly expressed in the cytoplasm (Fig. 3B). Subsequently, an RNA immunoprecipitation assay was performed to determine whether Ago2, a key component of the RNA-induced silencing complex, may combine with lnc-RGS5 and further mediate the binding of miRNAs with lnc-RGS5. Results of the present study demonstrated the significant enrichment of lnc-RGS5 immunoprecipitated by the anti-Ago2 antibody, compared

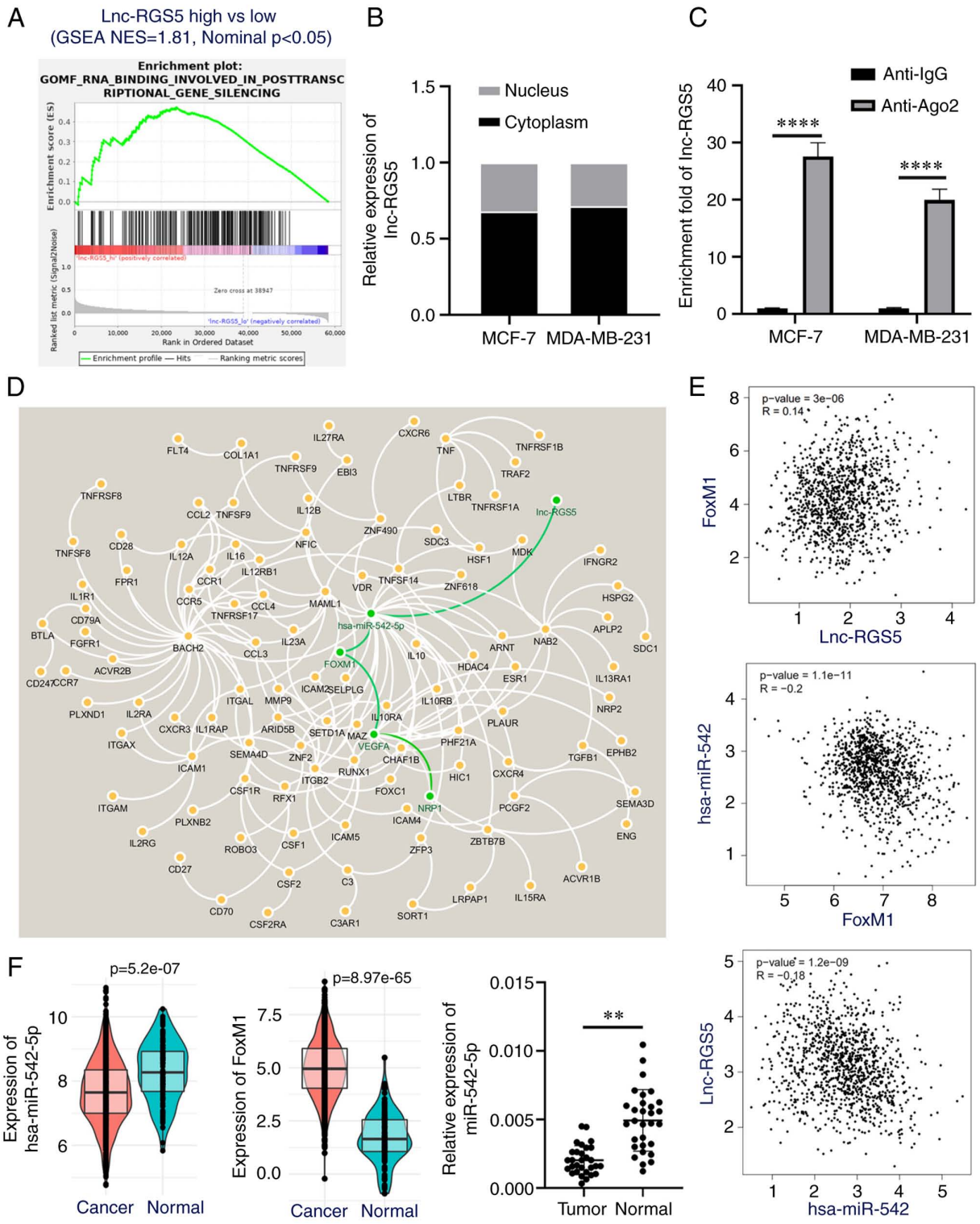

Figure 3. Identification of the lnc-RGS5/miR-542-5p/FoxM1 axis. (A) GSEA of Gene Ontology functions in high and low lnc-RGS5 expression groups. (B) Expression of lnc-RGS5 in the nucleus and cytoplasm. (C) Enrichment of lnc-RGS5 via anti-Ago2 immunoprecipitation compared with anti-IgG. (D) Network analysis of lnc-RGS5 in BRCA based on putative interactions. (E) Expression correlation analysis between FoxM1 and lnc-RGS5, FoxM1 and miR-542-5p, and lnc-RGS5 and miR-542-5p in BRCA. (F) Expression of miR-542-5p and FoxM1 in BRCA tissue samples from TCGA (left). Reverse transcription-quantitative PCR analysis of miR-542-5p expression in BRCA tissues and healthy samples (right; n=30). **P<0.01 and ****P<0.0001. lncRNA, long non-coding RNA; miRNA, microRNA; FoxM1, forkhead box M1; GSEA, gene set enrichment analysis; BRCA, breast cancer; RGS5, regulator of G protein signaling 5; TCGA, The Cancer Genome Atlas.

with anti-IgG (Fig. 3C). Collectively, results of the present study indicated that lnc-RGS5 may function as a ceRNA.

A ceRNA regulation network of lnc-RGS5 was subsequently constructed based on an integrative analysis (Fig. 3D). Results of the present study demonstrated that miR-542-5p (degree; 26) was the potential target of lnc-RGS5. *VEGFA* was the hub gene (degree; 15) of the downstream network regulated by miR-542-5p/*FoxM1* signaling. *NRP1* was one of the receptors of

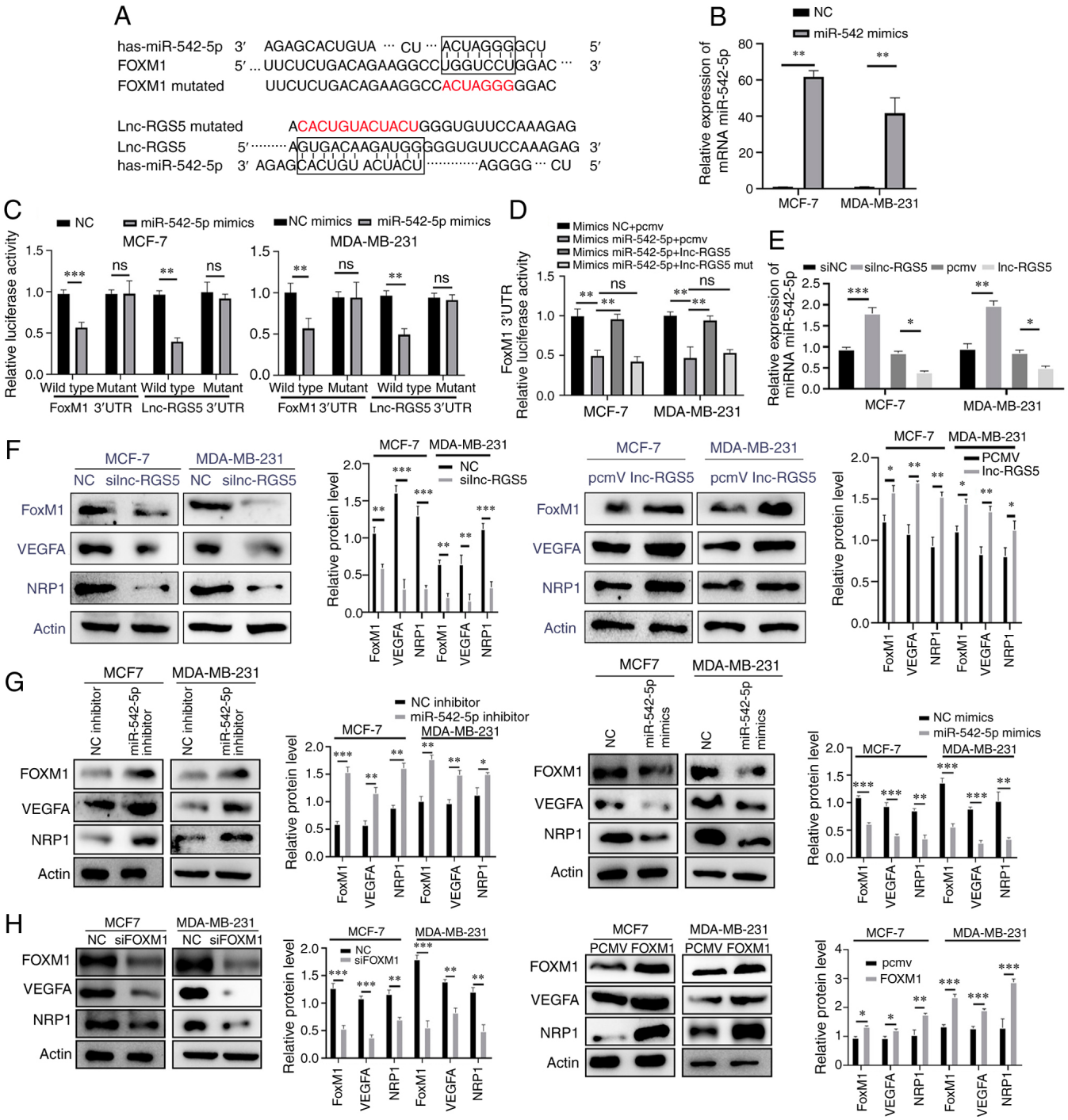

Figure 4. lnc-RGS5 acts as a ceRNA to promote BRCA cell proliferation *in vitro*. (A) The mutation sites of lnc-RGS5 and FoxM1 that bind to miR-542-5p. (B) Transfection efficiency of miR-542 mimics in MCF-7 and MDA-MB-231 cells. (C) Relative luciferase activity of lnc-RGS5, lnc-RGS5-Mut, FoxM1 and FoxM1-Mut in BRCA cells co-transfected with miR-542-5p. (D) Dual-luciferase assays indicated that lnc-RGS5 overexpression plasmid, but not lnc-RGS5-Mut, reversed the miR-542-5p overexpression-mediated decreased luciferase activity of FoxM1 3'UTR. (E) Expression of miR-542-5p following lnc-RGS5 transfection. (F-H) Expression of FoxM1 and VEGFA/NRP1 following lnc-RGS5, miR-542-5p or FoxM1 transfection in BRCA cells. *P<0.05, **P<0.01 and ***P<0.001. PCMV, pcDNA3,1 empty vector; lncRNA, long non-coding RNA; ceRNA, competing endogenous RNA; BRCA, breast cancer; FoxM1, forkhead box M1; miRNA, microRNA; Mut, mutant; RGS5, regulator of G protein signaling 5; UTR, untranslated region; NRP1, Neuropilin 1; NC, negative control.

ligand *VEGFA*. Moreover, expression correlation analysis revealed that miR-542-5p was negatively correlated with lnc-RGS5 and *FoxM1*, while lnc-RGS5 was positively correlated with *FoxM1* in BRCA (P<0.05; Fig. 3E). In addition, miR-542-5p was downregulated and *FoxM1* was upregulated in BRCA, compared with healthy samples (Fig. 3F). These results were consistent with those demonstrating the ceRNA mechanism.

Subsequently, the binding sites of miR-542-5p on lnc-RGS5 and *FoxM1* were mutated (Fig. 4A), and miR-542-5p was overexpressed following transfection with the miRNA mimics (Fig. 4B). Results of the dual-luciferase assay indicated that miR-542-5p significantly reduced the luciferase activity of lnc-RGS5 and *FoxM1* in BRCA cells. However, no significant differences in the luciferase activity of lnc-RGS5-Mut and

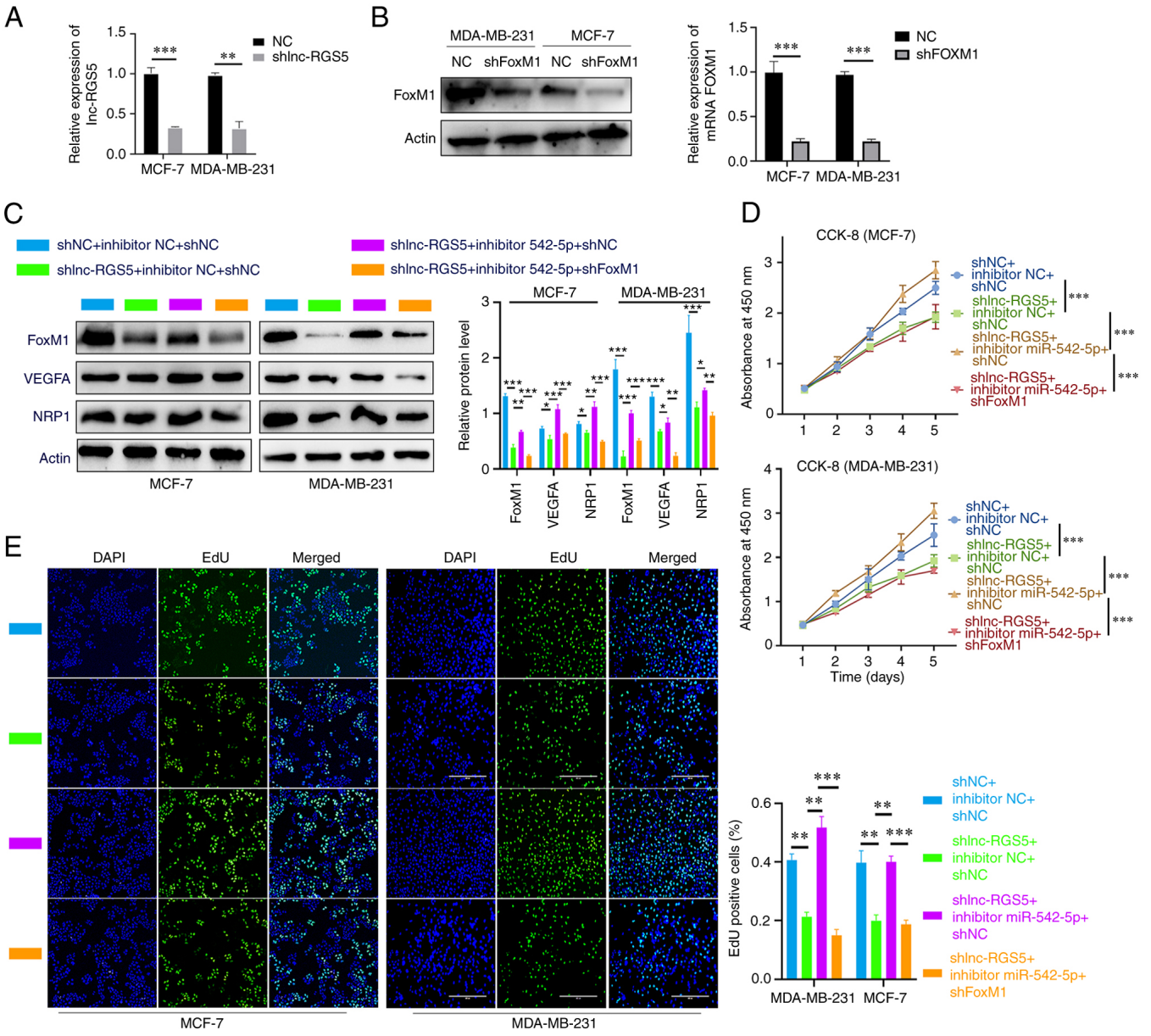

Figure 5. lnc-RGS5 promotes BRCA cell growth through miR-542-5p/FoxM1 *in vitro*. (A and B) Transfection efficiency of shlnc-RGS5 and shFoxM1. (C) Western blot analysis indicated that inhibitor-542-5p rescued shlnc-RGS5-mediated inhibition of FoxM1 and VEGFA/NRP1 expression in BRCA cells, and this was reversed following FoxM1 knockdown. (D and E) EdU and CCK-8 assays indicated that inhibitor-542-5p rescued the shlnc-RGS5-mediated inhibition of BRCA cell proliferation, and this was reversed following FoxM1 knockdown. *P<0.05, **P<0.01 and ***P<0.001. lncRNA, long non-coding RNA; BRCA, breast cancer; miRNA, microRNA; FoxM1, forkhead box M1; shRNA, short hairpin RNA; RGS5, regulator of G protein signaling 5; NRP1, Neuropilin 1; CCK-8, Cell Counting Kit-8; NC, negative control.

FoxM1-Mut were observed following miR-542-5p overexpression (Fig. 4C). Notably, transfection with the lnc-RGS5 overexpression vector reversed the decreased pmirGLO-FoxM1 3'UTR luciferase activity induced by miR-542-5p; however, this was not observed with the lnc-RGS5-Mut in which the miR-542-5p binding site was mutated (Fig. 4D). Collectively, these results demonstrated that miR-542-5p directly binds to lnc-RGS5 and *FoxM1*.

lnc-RGS5 promotes BRCA cell proliferation through the miR-542-5p/FoxM1 axis in vitro. Results of the RT-q-PCR analysis revealed that miR-542-5p was upregulated in silnc-RGS5 cells compared with siNC cells, while miR-542-5p was downregulated in cells overexpressing lnc-RGS5, compared with those transfected with the empty vector (Fig. 4E). Transfection with the lnc-RGS5 overexpression vector or miR-542-5p inhibitor upregulated the expression of *FoxM1* and *VEGFA/NRP1*, while transfection with si-lnc-RGS5 or miR-542-5p mimics downregulated the corresponding expression (Fig. 4F and G). Moreover, *FoxM1* overexpression promoted the expression of *VEGFA/NRP1*, while transfection with si*FoxM1* inhibited the corresponding expression (Fig. 4H). Subsequently, the efficiency of shlnc-RGS5 and shFoxM1 transfection was determined (Fig. 5A and B). The decreased proliferative ability and *FoxM1/VEGFA/NRP1* expression induced by sh*lnc-RGS5* were regained following co-transfection with the miR-542-5p inhibitor. Notably, these results were inhibited following

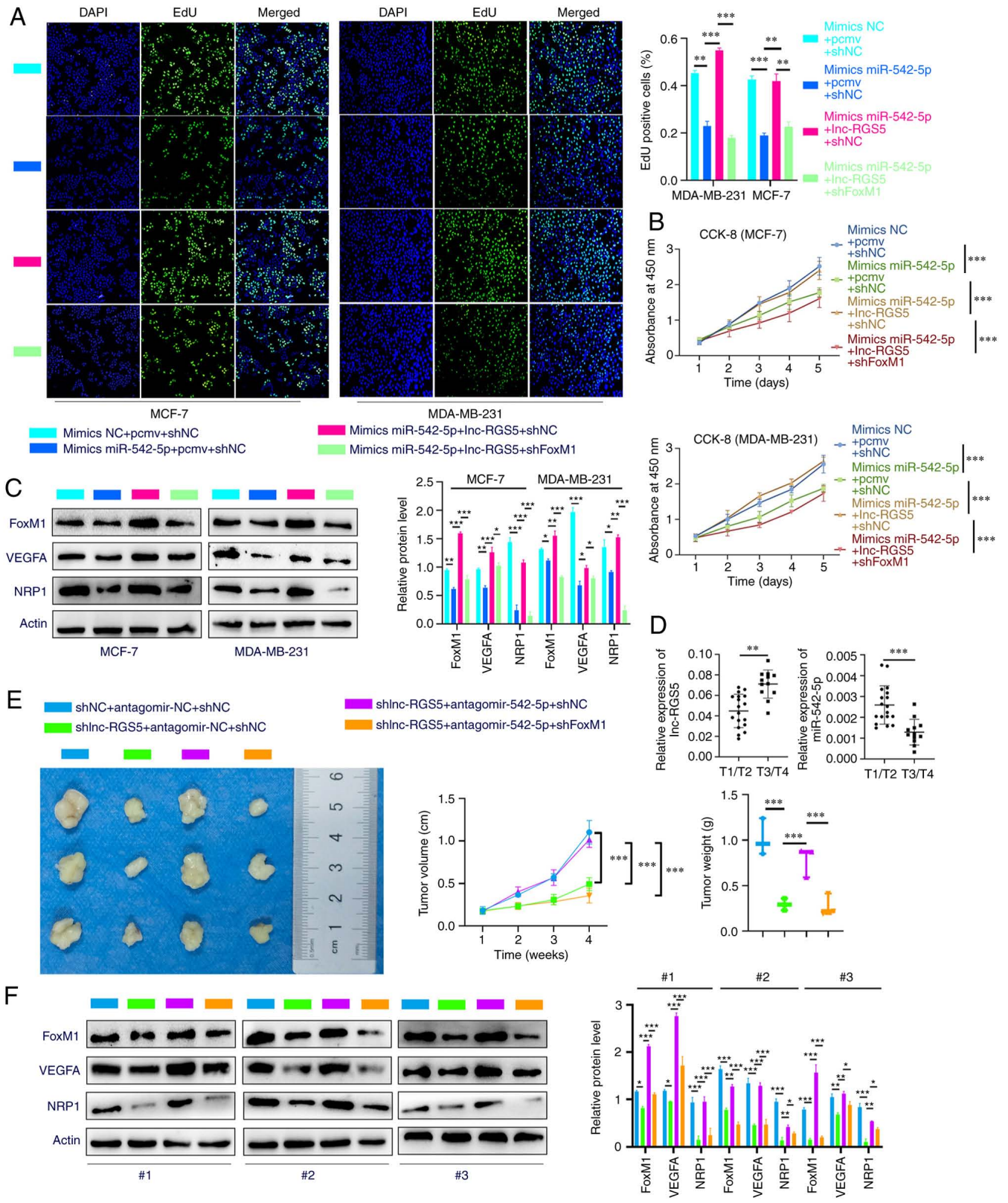

Figure 6. lnc-RGS5 promotes BRCA cell growth through miR-542-5p/FoxM1 *in vitro* and *in vivo*. (A and B) EdU and CCK-8 assays indicated that lnc-RGS5 rescued the miR-542-5p mimics-mediated inhibition of BRCA cell proliferation, and this was reversed following FoxM1 knockdown. (C) Western blot assays indicated that lnc-RGS5 rescued the miR-542-5p mimics-mediated inhibition of FoxM1 and VEGFA/NRP1 expression in BRCA cells, and this was reversed following FoxM1 knockdown. (D) Relative expression of lnc-RGS5 and miR-542-5p between T3/T4 and T1/T2 BRCA tissues. (E) Treatment with antagomir-542-5p rescued the shlnc-RGS5-mediated inhibition of BRCA cell growth, and this was reversed following FoxM1 knockdown. (F) Western blot assays of xenograft-derived tissues indicated that antagomir-542-5p treatment rescued the shlnc-RGS5-mediated inhibition of FoxM1 and VEGFA/NRP1 expression in BRCA cells, and this was reversed following FoxM1 knockdown. MDA-MB-231 cells stably expressing LV-shlnc-RGS5 or LV-NC were used for *in vivo* experiments. T1/T2, maximum tumor diameter was ≤5 cm; T3/T4, maximum tumor diameter was >5 cm. *P<0.05, **P<0.01 and ***P<0.001. PCMV, pcDNA3.1 empty vector; lncRNA, long non-coding RNA; BRCA, breast cancer; miRNA, microRNA; FoxM1, forkhead box M1; CCK-8, Cell Counting Kit-8; NRP1, Neuropilin 1; RGS5, regulator of G protein signaling 5; shRNA, short hairpin RNA; NC, negative control; LV, lentiviral vector; NC, negative control.

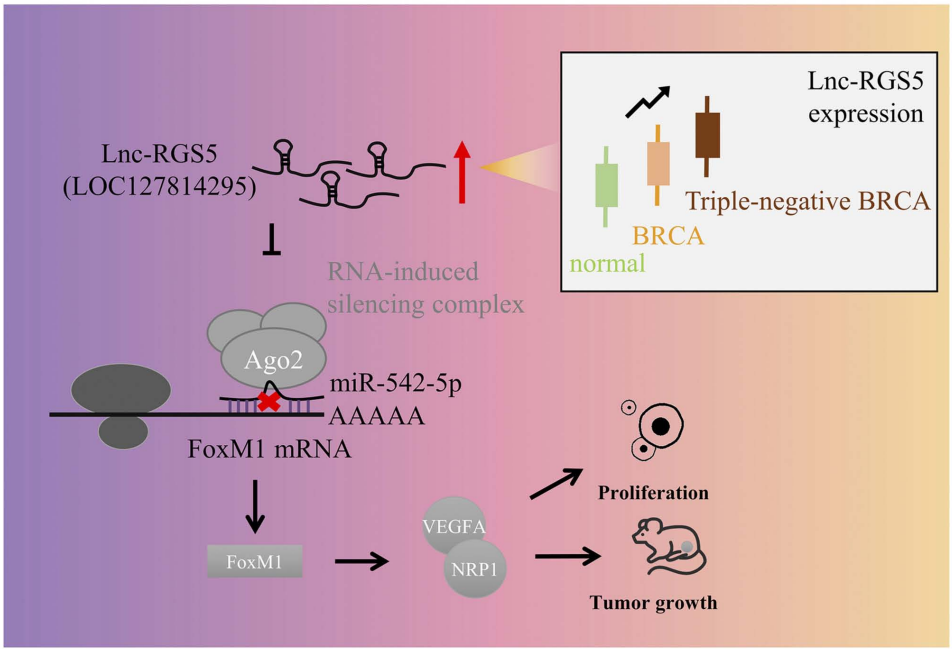

Figure 7. Mechanistic role of lnc-RGS5 in promoting BRCA cell growth. lnc-RGS5 acts as a ceRNA that sponges miR-542-5p to promote BRCA cell proliferation *in vitro* and *in vivo*. lncRNA, long non-coding RNA; BRCA, breast cancer; lnc-RGS5, lncRNA regulator of G protein signaling 5; ceRNA, competing endogenous RNA; miRNA, microRNA.

transfection with sh*FoxM1* in BRCA cells (Fig. 5C-E). The decreased proliferative ability and protein expression levels of *FoxM1*/*VEGFA*/*NRP1* induced by miR-542-5p mimics were regained following co-transfection with lnc-RGS5. Notably, these results were inhibited following transfection with sh*FoxM1* in BRCA cells (Fig. 6A-C). Thus, lnc-RGS5 competitively sponges miR-542-5p to prevent miR-542-5p binding to *FoxM1* 3'UTRs, resulting in *FoxM1* upregulation and increased proliferation of BRCA cells.

lnc-RGS5 promotes BRCA cell proliferation through a ceRNA pattern in vivo. Analysis of BRCA tissues revealed that the expression of lnc-RGS5 was higher in patients with T3/T4 tumors compared with patients with T1/T2 tumors, while the expression of miR-542-5p was lower in patients with T3/T4 tumors compared with patients with T1/T2 tumors. Rescue experiments explored whether lnc-RGS5 exerts biological functions via a ceRNA pattern *in vivo*. Treatment with antagomir-542-5p significantly abolished the decreased tumor growth in LV-sh*lnc-RGS5* tumors, which was reversed following *FoxM1* knockdown (Fig. 6E). Results of the western blot analysis of xenograft tumors demonstrated that treatment with antagomir-542-5p recovered the decreased protein expression of *FoxM1*/*VEGFA*/*NRP1* in LV-shlnc-RGS5 tumors, and this was reduced following *FoxM1* knockdown (Fig. 6F). Collectively, these data demonstrated that lnc-RGS5 acts as a ceRNA for miR-542-5p to promote BRCA cell proliferation *in vitro* and *in vivo* (Fig. 7).

Discussion

Results of the present study demonstrated that lnc-RGS5 was upregulated in BRCA tissues compared with healthy samples and associated with the overall survival of patients with triple-negative BRCA. Functionally, lnc-RGS5 promoted the proliferation of BRCA cells *in vitro* and *in vivo*. Mechanistically, lnc-RGS5 functions by competitively sponging miR-542-5p to promote *FoxM1*/*VEGFA* signaling. Thus, lnc-RGS5 may exhibit potential as a novel target for the treatment of BRCA.

Results of the present study revealed that lnc-RGS5 may act as a cancer-associated lncRNA. Pathway and functional analyses demonstrated that lnc-RGS5 was involved in DNA replication and signaling pathways associated with cell proliferation, differentiation and metastasis, such as mTOR, MAPK and VEGF signaling pathways. However, clinical data analysis revealed that the expression of lnc-RGS5 was not significantly associated with lymph node or distant metastasis. Thus, the present study focused on the regulatory role of lnc-RGS5 in the proliferation of BRCA cells. Notably, results of the GSEA revealed that RNA binding involved in post-transcriptional gene silencing was the most significantly enriched molecular function. Thus, a ceRNA network was constructed to investigate the potential mechanistic role of lnc-RGS5.

Results of the present study demonstrated that lnc-RGS5 knockdown inhibited *FoxM1*/*VEGFA* signaling via ceRNA mechanisms, implying that lnc-RGS5 may act as an alternative target for combined therapy with anti-VEGFA therapies, as anti-VEGFA monotherapy stimulated higher *VEGF* expression in BRCA (6,7). lnc-RGS5 may also be involved in DNA repair pathways, such as mismatch repair, base/nucleotide excision repair and homologous recombination. DNA damage is a hallmark of cancer as it may lead to tumor evolution and microenvironment remodeling, which is consistent with the functional results of the present study, in which lnc-RGS5 was associated with immune-associated pathways, such

as FcγR-mediated phagocytosis. Further experiments are required to elucidate the molecular mechanisms underlying lnc-RGS5 in the tumor microenvironment.

FoxM1 transcription factor is a member of the forkhead box family. Results of a previous study revealed that *FoxM1* upregulation promoted BRCA tumorigenesis (23), and *VEGFA* and *NRP1* were also upregulated (24). However, the corresponding expression levels and roles in cell proliferation in BRCA were not further validated. *FoxM1* is a critical downstream effector of PI3K-AKT and JNK/MAPK signaling pathways for cell proliferation, cell cycle control and DNA damage repair (25). Results of the present study revealed that *FoxM1* may also be regulated by lnc-RGS5/miR-542-5p signaling to promote cell proliferation. *FOXM1* is involved in three main cellular mechanisms of single-strand break repair; namely, nucleotide excision repair, base excision repair and mismatch repair (26). For example, *FoxM1* transcriptionally promotes the expression of replication factor c subunit 5 to participate in nucleotide excision repair (27). Notably, results of the present study revealed the potential function of lnc-RGS5 in the regulation of DNA damage repair through regulating *FoxM1*. In addition, results of a previous study indicated that *FoxM1* may exhibit potential as a target in the treatment of tumors (25). However, transcription factors are complex drug targets due to disordered structures and a lack of significant small molecule binding pockets (28). A previous study revealed an alternative approach to targeting transcription factors; for example, targeting the upstream non-coding RNA. Specifically, targeting lncRNA H19 inhibited *FoxM1* in gallbladder cancer (29). Thus, lnc-RGS5 may act as a novel upstream target to suppress *FoxM1* and *VEGFA*.

Results of a previous study revealed that the *VEGFA/NRP1* axis may regulate cell proliferation in BRCA (30). Notably, autocrine *VEGFA* produced by tumor cells promoted tumor-forming capacity *in vivo*, independent of effects on angiogenesis through interaction with NRP1 (30). Considering the effect of VEGFA in angiogenesis with VEGF receptor-1/2 (31), VEGFA may promote cell growth through activating both VEGFR-1/2 and NRP1/Ras signaling pathways in BRCA. Future studies are required to determine whether lnc-RGS5 promotes BRCA cell growth via angiogenesis *in vivo*. Moreover, in future studies, more animals will be used for *in vivo* experiments.

As a tumor suppressor gene, miR-542-5p plays an important role in various tumors (32). miR-542-5p promotes the progression of BRCA through inhibiting Ubiquitin Specific Peptidase 17 Like Family Member 2 (USP17L2, also known as DUB3), and treatment with pristimerin reversed this process at the cellular level (32). Results of a previous study also demonstrated that miR-542-5p inhibits tumor progression in lung cancer through inhibiting EGFR (33). Thus, lnc-RGS5 may exhibit potential as a targeted therapeutic drug to supplement pristimerin, or as a target of combined therapy.

In conclusion, results of the present study revealed that lnc-RGS5 may act as a novel oncogenic lncRNA in BRCA, and may exhibit potential in the treatment of BRCA.

Acknowledgements

Not applicable.

Funding

The present study was supported by Key Research and Development of Social and People's Livelihood (grant nos.cstc2018jscx-mszdX0031 and CSTC510215195605120418).

Availability of data and materials

The datasets used and/or analyzed during the current study are available from TCGA (https://portal.gdc.cancer.gov/).

Authors' contributions

JS, YT and FS were responsible for conceptualization. JS and YT were responsible for the methodology. JS was responsible for software and validation. JS and YT were responsible for normal analysis, and JS was responsible for investigation. JS was responsible for resources, data curation and writing the original draft. JS and YT were responsible for reviewing and editing. JS was responsible for visualization. FS was responsible for supervision. FS was responsible for project administration and funding acquisition. JS and YT confirm the authenticity of all the raw data. All authors read and approved the final version of the manuscript.

Ethics approval and consent to participate

All animal experiments were reviewed and approved (approval no. IACUC-CQMU-2022-0016) by the Experimental Animal Management and Use Committee of Chongqing Medical University (Chongqing, China). Informed consent was obtained from all patients. All experimental procedures were approved by Chongqing Medical University.

Patient consent for publication

Not applicable.

Competing interests

The authors declare that they have no competing interests.

References

1. Siegel RL, Miller KD, Wagle NS and Jemal A: Cancer statistics, 2023. CA Cancer J Clin 73: 17-48, 2023.
2. Denkert C, Liedtke C, Tutt A and von Minckwitz G: Molecular alterations in triple-negative breast cancer-the road to new treatment strategies. Lancet 389: 2430-2442, 2017.
3. Li Y, Zhang H, Merkher Y, Chen L, Liu N, Leonov S and Chen Y: Recent advances in therapeutic strategies for triple-negative breast cancer. J Hematol Oncol 15: 121, 2022.
4. Murphy CG: The Role of CDK4/6 inhibitors in breast cancer. Curr Treat Options Oncol 20: 52, 2019.
5. Kim C, Gao R, Sei E, Brandt R, Hartman J, Hatschek T, Crosetto N, Foukakis T and Navin NE: Chemoresistance Evolution in triple-negative breast cancer delineated by single-cell sequencing. Cell 173: 879-893.e13, 2018.
6. Gupta GK, Collier AL, Lee D, Hoefer RA, Zheleva V, Siewertsz van Reesema LL, Tang-Tan AM, Guye ML, Chang DZ, Winston JS, *et al*: Perspectives on triple-negative breast cancer: Current treatment strategies, unmet needs, and potential targets for future therapies. Cancers (Basel) 12: 2392, 2020.

7. Mahdi A, Darvishi B, Majidzadeh AK, Salehi M and Farahmand L: Challenges facing antiangiogenesis therapy: The significant role of hypoxia-inducible factor and MET in development of resistance to anti-vascular endothelial growth factor-targeted therapies. J Cell Physiol 234: 5655-5663, 2019.
8. Wang J, Xie S, Yang J, Xiong H, Jia Y, Zhou Y, Chen Y, Ying X, Chen C, Ye C, *et al*: The long noncoding RNA H19 promotes tamoxifen resistance in breast cancer via autophagy. J Hematol Oncol 12: 81, 2019.
9. Lu G, Li Y, Ma Y, Lu J, Chen Y, Jiang Q, Qin Q, Zhao L, Huang Q, Luo Z, *et al*: Long noncoding RNA LINC00511 contributes to breast cancer tumourigenesis and stemness by inducing the miR-185-3p/E2F1/Nanog axis. J Exp Clin Cancer Res 37: 289, 2018.
10. Shahi P, Wang CY, Chou J, Hagerling C, Gonzalez Velozo H, Ruderisch A, Yu Y, Lai MD and Werb Z: GATA3 targets semaphorin 3B in mammary epithelial cells to suppress breast cancer progression and metastasis. Oncogene 36: 5567-5575, 2017.
11. Zhang M, Wang N, Song P, Fu Y, Ren Y, Li Z and Wang J: LncRNA GATA3-AS1 facilitates tumour progression and immune escape in triple-negative breast cancer through destabilization of GATA3 but stabilization of PD-L1. Cell Prolif 53: e12855, 2020.
12. Dasgupta S, Ghosh T, Dhar J, Bhuniya A, Nandi P, Das A, Saha A, Das J, Guha I, Banerjee S, *et al*: RGS5-TGFβ-Smad2/3 axis switches pro- to anti-apoptotic signaling in tumor-residing pericytes, assisting tumor growth. Cell Death Differ 28: 3052-3076, 2021.
13. Silini A, Ghilardi C, Figini S, Sangalli F, Fruscio R, Dahse R, Pedley RB, Giavazzi R and Bani M: Regulator of G-protein signaling 5 (RGS5) protein: A novel marker of cancer vasculature elicited and sustained by the tumor's proangiogenic microenvironment. Cell Mol Life Sci 69: 1167-1178, 2012.
14. Boss CN, Grünebach F, Brauer K, Häntschel M, Mirakaj V, Weinschenk T, Stevanovic S, Rammensee HG and Brossart P: Identification and characterization of T-cell epitopes deduced from RGS5, a novel broadly expressed tumor antigen. Clin Cancer Res 13: 3347-3355, 2007.
15. Love MI, Huber W and Anders S: Moderated estimation of fold change and dispersion for RNA-seq data with DESeq2. Genome Biol 15: 550, 2014.
16. Subramanian A, Tamayo P, Mootha VK, Mukherjee S, Ebert BL, Gillette MA, Paulovich A, Pomeroy SL, Golub TR, Lander ES and Mesirov JP: Gene set enrichment analysis: A knowledge-based approach for interpreting genome-wide expression profiles. Proc Natl Acad Sci USA 102: 15545-15550, 2005.
17. Krüger J and Rehmsmeier M: RNAhybrid: MicroRNA target prediction easy, fast and flexible. Nucleic Acids Res 34 (Web Server Issue): W451-W454, 2006.
18. Enright AJ, John B, Gaul U, Tuschl T, Sander C and Marks DS: MicroRNA targets in Drosophila. Genome Biol 5: R1, 2003.
19. Yevshin I, Sharipov R, Valeev T, Kel A and Kolpakov F: GTRD: A database of transcription factor binding sites identified by ChIP-seq experiments. Nucleic Acids Res 45 (D1): D61-D67, 2017.
20. Livak KJ and Schmittgen TD: Analysis of relative gene expression data using real-time quantitative PCR and the 2(-Delta Delta C(T)) method. Methods 25: 402-408, 2001.
21. Wang S, Zhen L, Liu Z, Ai Q, Ji Y, Du G, Wang Y and Bu Y: Identification and analysis of the promoter region of the human HAS3 gene. Biochem Biophys Res Commun 460: 1008-1014, 2015.
22. Tian Y, Ma R, Sun Y, Liu H, Zhang H, Sun Y, Liu L, Li Y, Song L and Gao P: SP1-activated long noncoding RNA lncRNA GCMA functions as a competing endogenous RNA to promote tumor metastasis by sponging miR-124 and miR-34a in gastric cancer. Oncogene 39: 4854-4868, 2020.
23. Yang C, Chen H, Yu L, Shan L, Xie L, Hu J, Chen T and Tan Y: Inhibition of FOXM1 transcription factor suppresses cell proliferation and tumor growth of breast cancer. Cancer Gene Ther 20: 117-124, 2013.
24. Luo M, Hou L, Li J, Shao S, Huang S, Meng D, Liu L, Feng L, Xia P, Qin T and Zhao X: VEGF/NRP-1axis promotes progression of breast cancer via enhancement of epithelial-mesenchymal transition and activation of NF-κB and β-catenin. Cancer Lett 373: 1-11, 2016.
25. Yao S, Fan LYN and Lam EWF: The FOXO3-FOXM1 axis: A key cancer drug target and a modulator of cancer drug resistance. Semin Cancer Biol 50: 77-89, 2018.
26. Kalathil D, John S and Nair AS: FOXM1 and cancer: Faulty cellular signaling derails homeostasis. Front Oncol 10: 626836, 2021.
27. Peng WX, Han X, Zhang CL, Ge L, Du FY, Jin J and Gong AH: FoxM1-mediated RFC5 expression promotes temozolomide resistance. Cell Biol Toxicol 33: 527-537, 2017.
28. Bushweller JH: Targeting transcription factors in cancer-from undruggable to reality. Nat Rev Cancer 19: 611-624, 2019.
29. Wang SH, Ma F, Tang ZH, Wu XC, Cai Q, Zhang MD, Weng MZ, Zhou D, Wang JD and Quan ZW: Long non-coding RNA H19 regulates FOXM1 expression by competitively binding endogenous miR-342-3p in gallbladder cancer. J Exp Clin Cancer Res 35: 160, 2016.
30. Cao Y, E G, Wang E, Pal K, Dutta SK, Bar-Sagi D and Mukhopadhyay D: VEGF exerts an angiogenesis-independent function in cancer cells to promote their malignant progression. Cancer Res 72: 3912-3918, 2012.
31. Simons M, Gordon E and Claesson-Welsh L: Mechanisms and regulation of endothelial VEGF receptor signalling. Nat Rev Mol Cell Biol 17: 611-625, 2016.
32. Cheng S, Zhang Z, Hu C, Xing N, Xia Y and Pang B: Pristimerin suppressed breast cancer progression via miR-542-5p/DUB3 axis. Onco Targets Ther 13: 6651-6660, 2020.
33. He RQ, Li XJ, Liang L, Xie Y, Luo DZ, Ma J, Peng ZG, Hu XH and Chen G: The suppressive role of miR-542-5p in NSCLC: The evidence from clinical data and in vivo validation using a chick chorioallantoic membrane model. BMC Cancer 17: 655, 2017.